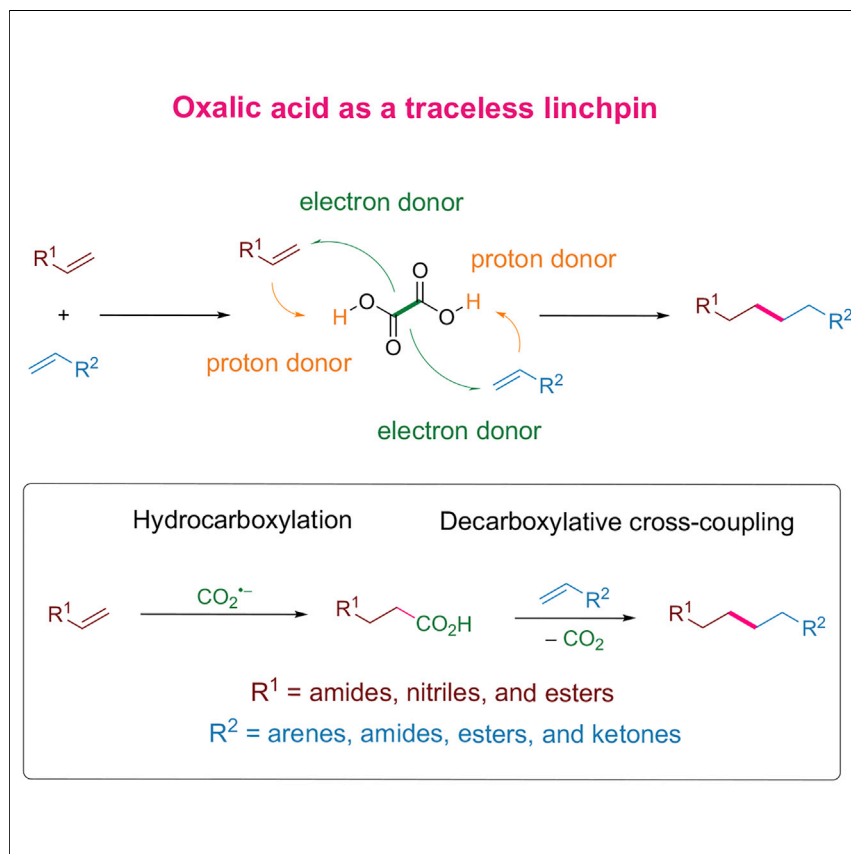


Article

Photocatalytic coupling of electron-deficient alkenes using oxalic acid as a traceless linchpin



Alkene cross-coupling is a straightforward strategy to construct C–C bonds between alkene feedstocks. We developed a reductive alkene coupling method utilizing oxalic acid as a traceless linchpin. The overall process is a two-step transformation involving hydrocarboxylation and decarboxylative cross-coupling. The synthetic utility was demonstrated by syntheses of two bioactive molecules. This article paves the way for the broad utilization of the reactive CO_2 radical anion intermediate in the synthesis of fine chemicals.

Zugen Wu, Mingyue Wu, Kun Zhu, Jie Wu, Yixin Lu

chmjie@nus.edu.sg (J.W.)
chmlyx@nus.edu.sg (Y.L.)

Highlights

Oxalic acid is used as a traceless linchpin

CO_2 radical anion formation via photocatalytic oxidation of oxalic acid is achieved

Homo- and cross-coupling of electron-poor alkenes is achieved



Article

Photocatalytic coupling of electron-deficient alkenes using oxalic acid as a traceless linchpin

Zugen Wu,¹ Mingyue Wu,¹ Kun Zhu,^{1,2} Jie Wu,^{1,3,*} and Yixin Lu^{1,2,4,*}

SUMMARY

Reductive alkene cross-coupling represents a straightforward strategy for the construction of C–C bonds from readily available alkene feedstocks. A one-pot protocol, utilizing oxalic acid as a traceless linchpin, has been developed to achieve direct cross-coupling of electron-deficient alkenes. The overall process is a two-step transformation involving hydrocarboxylation followed by decarboxylative cross-coupling. A dual-photocatalyst system is crucial for success and promotes the two reaction steps synergistically. This reaction supports the efficient synthesis of bioactive molecules. Photoredox catalysis provides an easy and mild pathway for the generation of a CO₂ radical anion from oxalic acid, which paves the way for the broad utilization of this reactive intermediate in the synthesis of fine chemicals.

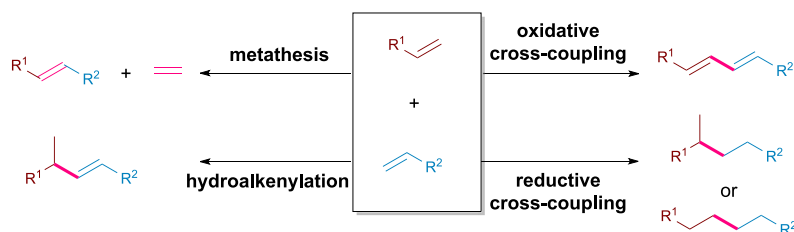
INTRODUCTION

Formation of C–C bonds is fundamentally important in organic chemistry, and consequently, the development of new strategies for the construction of C–C bonds is always an area of intensive research. Alkenes are the most readily available, abundant feedstocks available to the chemical industry, and numerous remarkably powerful synthetic strategies in organic chemistry make use of alkene substrates. The electrodimerization of acrylonitrile to adiponitrile, a precursor of nylon 6,6, is the largest industrial organic electrosynthetic process, accounting for around 30% of the annual global production of adiponitrile.¹ Olefin metathesis reactions exchange alkylidene moieties between alkenes and form new C–C double bonds.^{2,3} When terminal alkenes are employed in metathesis, internal alkenes and ethylene are formed. Alkene cross-coupling reactions are another group of useful transformations that connect two different alkene reaction partners as shown in Figure 1A. Typically, the redox-neutral alkene cross-coupling is known as hydroalkenylation.⁴ When ethylene is used as a reaction partner, hydrovinylation was realized with excellent regioselectivities and enantioselectivities under transition metal catalysis.^{5,6} Acrylates are often used as a reaction partner in the transition-metal-catalyzed oxidative cross-coupling reactions of alkenes, which form 1,3-diene products, and good *E/Z* selectivity has been achieved in certain cases.^{7–12} In the reductive cross-coupling of alkenes (Figure 1B), unsaturated olefin sites in the substrates are linked together to form fully saturated carbon skeletons. In their elegant studies, the Baran group accomplished functionalized alkene cross-coupling for the construction of C–C bonds by utilizing an iron catalyst with an inexpensive silane, and the reaction favored the formation of Markovnikov products.^{13,14} In a titanium(III)-catalyzed redox umpolung strategy, Streuff achieved reductive cross-coupling of enones with acrylonitriles.¹⁵ Very recently, Jiang and co-workers reported the enantioselective cross-coupling of α -branched vinylketones with vinylazaarenes, a reaction which involves cooperative photoredox and chiral hydrogen-bonding catalysis.¹⁶ With the

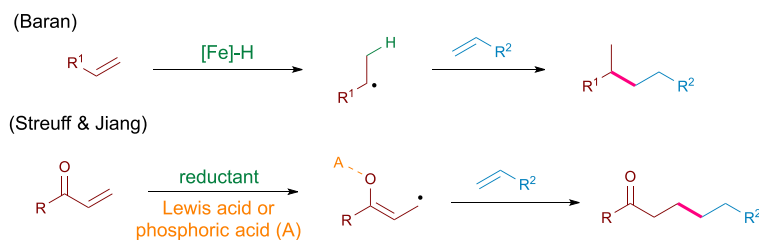
THE BIGGER PICTURE

C–C bond formation between alkenes utilizes simple alkene building blocks to construct complex carbon skeletons and is one of the most powerful strategies in synthetic organic chemistry. Previous terminal-to-terminal reductive cross-coupling methods usually relied on the single-electron reduction of one coupling partner. However, application of this strategy to acrylamide substrates, which possess a highly negative reductive potential, is difficult. We utilized oxalic acid as a “traceless linchpin” to achieve cross-coupling of two electron-deficient alkene components in a head-to-head fashion. The CO₂ radical anion, which is difficult to generate from CO₂ due to its high reductive potential, can be easily accessed from oxalic acid through mild photoredox catalysis. Considering the rich chemistry of carboxylic acid intermediates, we believe that oxalic acid can serve as a traceless linchpin in transformations beyond alkene couplings.

A Strategies for the construction of new C–C bonds from alkenes



B Reported reductive cross-coupling of alkenes



C This work: oxalic acid as a traceless linchpin

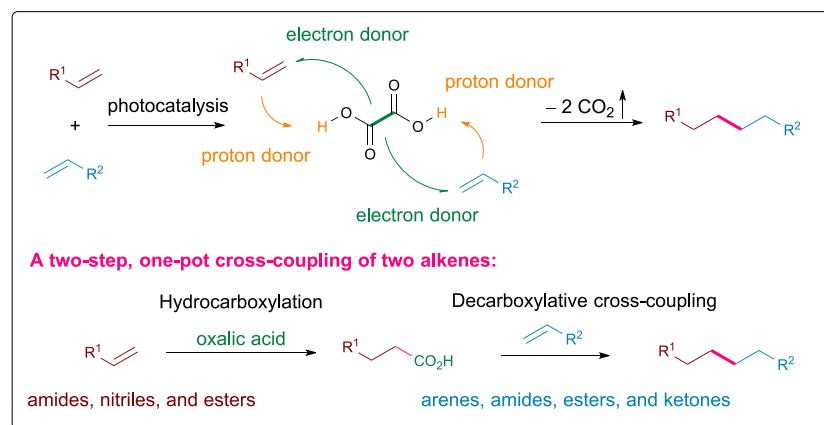


Figure 1. The construction of C–C bonds from alkene substrates

(A) Strategies for the construction of new C–C bonds from alkenes.

(B) Reported reductive cross-coupling of alkenes.

(C) This work: oxalic acid as a traceless linchpin.

ready availability and ubiquitous presence of alkenes in the chemical industry and the importance of C–C bond formation in organic synthesis, efficient methods for alkene cross-coupling are in high demand and hold great promise to provide new strategies for molecular retrosynthesis. In this context, we embarked on a journey toward the development of the novel and practical alkene cross-coupling strategy that is described here.

Linchpin strategy is very useful in cross-coupling reactions, which connect two molecular scaffolds via a molecular linker.^{17–19} To develop a powerful synthetic strategy that can cross-couple two different simple alkene components, we envisioned that a suitable “traceless linchpin” is the key to such a process. For example, Young and Rovis utilized CO₂ as a traceless mediator for site-selective C(sp³)/C(sp²)-H arylation^{20,21} and α -alkylation of primary aliphatic amines,²² respectively. Recently, carboxylic acids have been widely exploited as radical precursors in decarboxylative

¹Department of Chemistry, National University of Singapore, Singapore 117543, Singapore

²Joint School of National University of Singapore and Tianjin University, International Campus of Tianjin University, Bin-hai New City, Fuzhou, Fujian 350207, China

³National University of Singapore (Suzhou) Research Institute, 377 Lin Quan Street, Suzhou Industrial Park, Suzhou, Jiangsu 215123, China

⁴Lead contact

*Correspondence: chmjie@nus.edu.sg (J.W.), chmlyx@nus.edu.sg (Y.L.)

<https://doi.org/10.1016/j.chempr.2022.12.013>

coupling reactions.^{23,24} In our search for a linker that could be used in practical alkene cross-coupling reactions, we posited that oxalic acid may serve as an ideal traceless linchpin (Figure 1C).

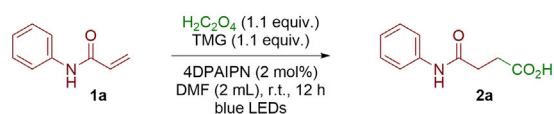
Oxalic acid, the simplest dicarboxylic acid, is not only a widely distributed metabolite in nature but also an abundant and low-cost feedstock (\$0.6/kg) in the industry, and it is readily produced from carbohydrates, olefins, carbon monoxide, or biomass.²⁵ The decarboxylative oxidation of oxalate generates a carbon dioxide radical anion ($\text{CO}_2^{\cdot-}$), which may effectively stitch two alkene reaction partners together. The carbon dioxide radical anion is a useful nucleophile and a strong reductant, but its access from the direct reduction of CO_2 requires a highly negative potential ($E_{1/2}(\text{CO}_2/\text{CO}_2^{\cdot-}) = -2.2$ V vs. SCE),²⁶ which hinders its utilization in synthetic chemistry.²⁷ Using the hydrogen atom abstraction from sodium formate as leverage, the groups of Jui and Wickens achieved the formation of a carbon dioxide radical anion and successfully utilized it in the single-electron reduction of an array of challenging substrates.^{26,28,29} With a low potential ($E_{1/2}(\text{C}_2\text{O}_4^{\cdot-}/\text{C}_2\text{O}_4^{2-}) = 0.06$ V vs. SCE),³⁰ the single-electron oxidation of oxalate represents an alternative strategy for the generation of carbon dioxide radical anion under mild conditions. Although it has been demonstrated that the electro-oxidation and photo-oxidation of oxalate generate the carbon dioxide radical anion,^{30,31} its use in synthetic chemistry has remained unexplored. For reaction development, we recognized the importance of applicability of the cross-coupling process to challenging but useful alkene substrates, such as α,β -unsaturated amides. Even though carbon dioxide radical anion is a potent reductant, it is unable to directly reduce α,β -unsaturated amides.²⁶ We thus devised a cascade photoredox reductive cross-coupling of alkenes with a two-step process. In the projected hydrocarboxylation step, the carbon dioxide radical anion produced by the decarboxylation of oxalate adds to an alkene, delivering a hydrocarboxylated intermediate. Subsequently, decarboxylation occurs to produce a terminal carbon-centered radical which, when added to another alkene reaction partner, eventually leads to the formation of the cross-coupling product. To facilitate the redox processes involved in these alkene cross-coupling reactions, we envisioned using a dual-photocatalyst system to activate oxalate and the carboxylate intermediate selectively. Herein, we report the utilization of oxalic acid as a linchpin for the cross-coupling of electron-deficient alkene substrates. The reaction is a photocatalytic process and forms a new C–C bond by efficiently linking two alkene substrates.

RESULTS AND DISCUSSION

Investigation of optimal reaction conditions

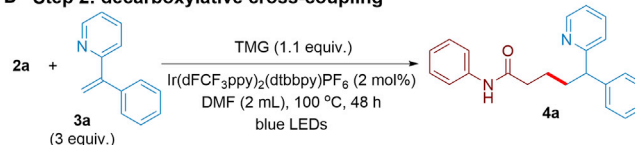
To commence our study, we carefully investigated the reaction conditions of both reaction steps. *N*-Phenyl acrylamide (**1a**) was chosen as the model substrate for the hydrocarboxylation reaction (Figure 2A). It was found that oxalic acid effectively promoted hydrocarboxylation in the presence of 1,1,3,3-tetramethylguanidine (TMG) and 1,3-dicyano-2,4,5,6-tetrakis-(diphenylamino)-benzene (4DPAIPN) in DMF at room temperature under blue-light irradiation, providing the desired hydrocarboxylated product (**2a**) with a yield of 62% (entry 1). When 4DPAIPN was replaced by a different photocatalyst, $\text{Ir}(\text{dFCF}_3\text{ppy})_2(\text{dtbbpy})\text{PF}_6$, the yield of **2a** dropped significantly to 32% (entry 2). Using cesium oxalate as the source of the carbon dioxide radical anion was less efficient due to its poor solubility, even when a mixture of DMF/water was used as the solvent, and **2a** was obtained with a yield of only 33% (entry 3). Control experiments showed that the reaction failed in the absence of the photocatalyst or light, suggesting that it is a photocatalytic process (entries 4

A Step 1: hydrocarboxylation



Entry	Variations to standard conditions	Yield ^a
1	none	62(57) ^b
2	Ir(dFCF ₃ ppy) ₂ (dtbbpy)PF ₆ instead of 4DPAIPN	32
3	Cs ₂ C ₂ O ₄ instead of H ₂ C ₂ O ₄ /TMG; DMF:H ₂ O = 5:1 as solvent	33
4	no photocatalyst	0
5	no light	0
6	r.t. for 12 h, and then 100 °C for 3 h	76

B Step 2: decarboxylative cross-coupling



Entry	Variations to standard conditions	Yield ^b
7	none	84
8	2 equiv. of 3; 24 h instead of 48 h	49
9	120 °C	61
10	4DPAIPN instead of Ir(dFCF ₃ ppy) ₂ (dtbbpy)PF ₆	0
11	no photocatalyst	0
12	no light	0

C One-pot cross-coupling protocol

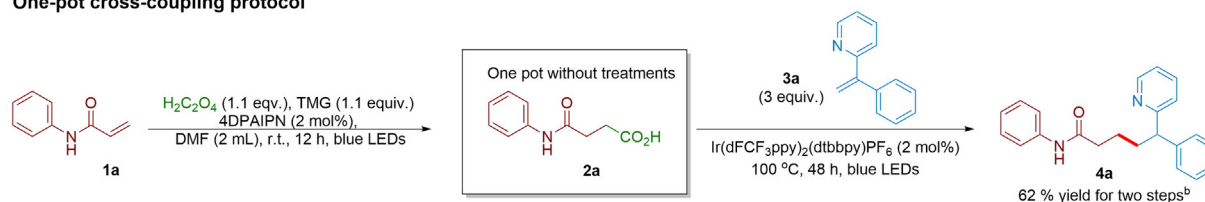


Figure 2. Optimization of reaction conditions

(A) Optimization of the hydrocarboxylation reaction.

(B) Optimization of the decarboxylative cross-coupling reaction.

(C) One-pot hydrocarboxylative and cross-coupling cascade. All reactions were conducted at 0.1 mmol scale. ^aRefers to ¹H NMR yields of methylated 2a. ^bRefers to isolated yields. Light emitting diode (LED).

and 5). When the reaction was performed at 100 °C, the chemical yield of the reaction was improved to 76% (entry 6).

For the subsequent decarboxylative cross-coupling step, we used 2-(1-phenylvinyl)pyridine (3a) as the coupling partner (Figure 2B). In the presence of Ir(dFCF₃ppy)₂(dtbbpy)PF₆ and TMG under blue-light irradiation at 100 °C, the desired cross-coupling product (4a) was isolated with a yield of 84% (entry 7). The structure of 4a was confirmed by single-crystal X-ray analysis (CCDC: 2193902). Decreasing the amount of 3a was detrimental to the reaction (entry 8), and increasing the temperature to 120 °C resulted in a decreased yield of 61% (entry 9). Although 4DPAIPN was the most effective photocatalyst for the hydrocarboxylation step, it was completely ineffective in the decarboxylative cross-coupling reaction (entry 10). These results suggested that 4DPAIPN is unable to oxidize the hydrocarboxylated intermediate. Similarly, control experiments confirmed that both photocatalyst and light are essential for this decarboxylative cross-coupling reaction (entries 11 and 12).

With the optimal conditions for both hydrocarboxylation and decarboxylative cross-coupling reaction steps in hand, we proceeded to establish the one-pot cross-coupling protocol (Figure 2C). Upon completion of the hydrocarboxylation reaction, the photocatalyst (Ir(dFCF₃ppy)₂(dtbbpy)PF₆) and the alkene (3a) were added directly, and the resulting mixture was heated to 100 °C. The decarboxylative cross-coupling reaction proceeded smoothly, and the desired cross-coupling product (4a) was isolated with a yield of 62%. It is worth noting that the combination of two reaction steps in one pot turned out to be more effective, with an overall yield higher than that obtained from the two reactions conducted separately. It is noteworthy that in the one-pot protocol, whether the hydrocarboxylation step is carried

out at room temperature or heated at 100°C, the overall yield of this two-step process remains the same, presumably because heating in the decarboxylative cross-coupling step promotes the conversion of acrylamide **1a** to acid **2a** in the hydrocarboxylation step.

Scope of alkene coupling reactions

With the optimal conditions in hand, the generality of the cross-coupling reaction of two different alkenes was investigated (Figure 3). The α,β -unsaturated amide (**1a**) smoothly cross-coupled with a range of α,α -biarylalkenes. When 2-pyridyl was one of these aryl moieties, the other aryl group, with a range of different *para*-substituents, ranging from simple halogen atoms (**4b–4d**) to an electron-withdrawing trifluoromethyl group (**4e**) or electron-donating methoxy/methyl groups (**4f** and **4g**), was tolerated well. The substitution pattern on this aryl moiety could also be varied (**4h**). In place of the 2-pyridyl moiety of alkene substrates, various substituted pyridines bearing a 6-methyl (**4i**), 5-fluoro (**4j**), or 4-chloro (**4k**) group were all found to be suitable, furnishing the desired coupling products in good yields. The pyridine moiety in the alkene structure could be replaced by other *N*-heteroarenes, for example, pyrazine (**4l**). A nitrogen-containing heterocycle in the alkene substrate is not an absolute requirement; when an α -phenyl-substituted acrylamide was used, the cross-coupling reaction with **1a** yielded a 1,6-diamide (**4m**) in moderate yield. Similarly, esters (**4n**) and ketones (**4o**) are both feasible substrates in this transformation, albeit with decreased efficiencies. The cross-coupling partners bearing no aryl substituents were also found to be suitable. When dehydroalanine was employed, an unnatural amino acid derivative (**4p**) was obtained in good yield. The Boc groups could be replaced by a phthalimide moiety (**4q**), although the reaction was less efficient. When electron-neutral alkenes such as diphenylethylenes were utilized, the desired cross-coupling products were formed, albeit in low yields (**4r–4t**). The employment of α -(trifluoromethyl)styrene delivered the *gem*-difluoroalkene (**4u**) with an isolated yield of only 16%.

The scope of α,β -unsaturated amide coupling partners was also evaluated. A range of *N*-phenyl acrylamides bearing various substituents at the *para*-position of the phenyl ring (**4v–4ac**) were found to be suitable. Notably, the ester substrate (**1ab**) was derived from benzocaine, an approved local anesthetic drug. Even though it was shown that carbon dioxide radical anion could reduce aryl halides,^{26,29} substrates bearing halogen atoms (**4v–4x**) were well tolerated in the cross-coupling reaction. The α,β -unsaturated amides bearing an alkyl or alkynyl substituent, with different substitution patterns, were all shown to be good reaction partners (**4ad–4af**); the C \equiv C triple bond remained intact during the reaction. Acrylamides containing a disubstituted phenyl ring also displayed good reactivity (**4ag**). The reaction scope was successfully extended to α -substituted acrylamides and *N*-phenyl acrylamides with an α -methyl (**4ah**), ethyl (**4ai**), benzyl (**4aj**), or phenyl (**4ak**) group, as all of them were found to be good coupling partners. Interestingly, this alkene cross-coupling reaction could be elaborated further into a domino process; when acrylamide containing an ester moiety at the α -position was utilized, a succinimide (**4al**) was obtained in moderate yield. Finally, the cross-coupling reaction was also applicable to α,β -unsaturated nitriles (**4am**, **4an**) and esters (**4ao**), even though the efficiency of such transformations was lower than that of α,β -unsaturated amide substrates.

We further examined the feasibility of the alkene homocoupling reaction using oxalic acid as a traceless linchpin. Different from the aforementioned acrylamides/acrylonitriles/acrylates ($E_{p/2}$ around -2.1 V vs. SCE), *N*-acryloyl-3,5-dimethylpyrazole

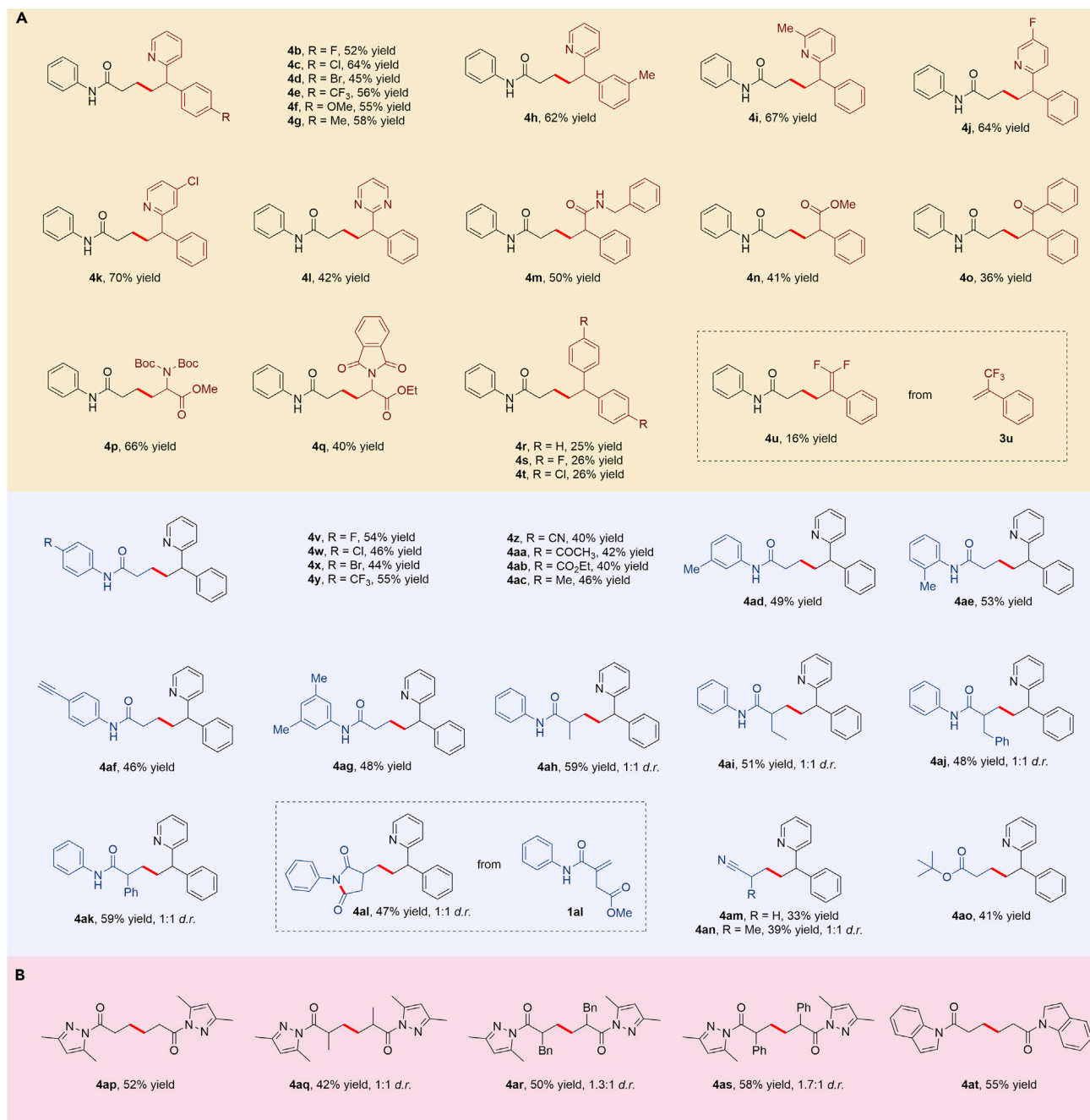


Figure 3. Reaction scopes of alkene cross-coupling

(A) Substrate scope for one-pot hydrocarboxylative and cross-coupling cascade.

(B) Scope for homocouplings. Reaction conditions are as follows: (1) for cross-couplings: acrylamides/acrylonitriles/acrylate (0.1 mmol), α,α -disubstituted alkenes (0.3 mmol), oxalic acid (0.11 mmol), TMG (0.11 mmol), 4DPAIPN (0.002 mmol), Ir(dFCF₃ppy)₂(dtbbpy)PF₆ (0.002 mmol), and DMF (2 mL). The reaction was irradiated under blue LEDs in a one-pot system: the hydrocarboxylation reaction was conducted at room temperature for 12 h, followed by decarboxylative cross-coupling at 100°C for 48 h. (2) For homocouplings: acrylamides (0.1 mmol), oxalic acid (0.055 mmol), TMG (0.055 mmol), 4DPAIPN (0.001 mmol), and DMF (1 mL). The reaction was irradiated under blue LEDs at room temperature for 12 h for isolated yields.

(1ap) displayed a strong tendency to homocoupling, probably because the transformation was selectively initiated by a single-electron reduction from CO₂^{•-} (E_{1/2}(CO₂/CO₂^{•-}) = -2.2 V vs. SCE) instead of the radical addition, in view of the

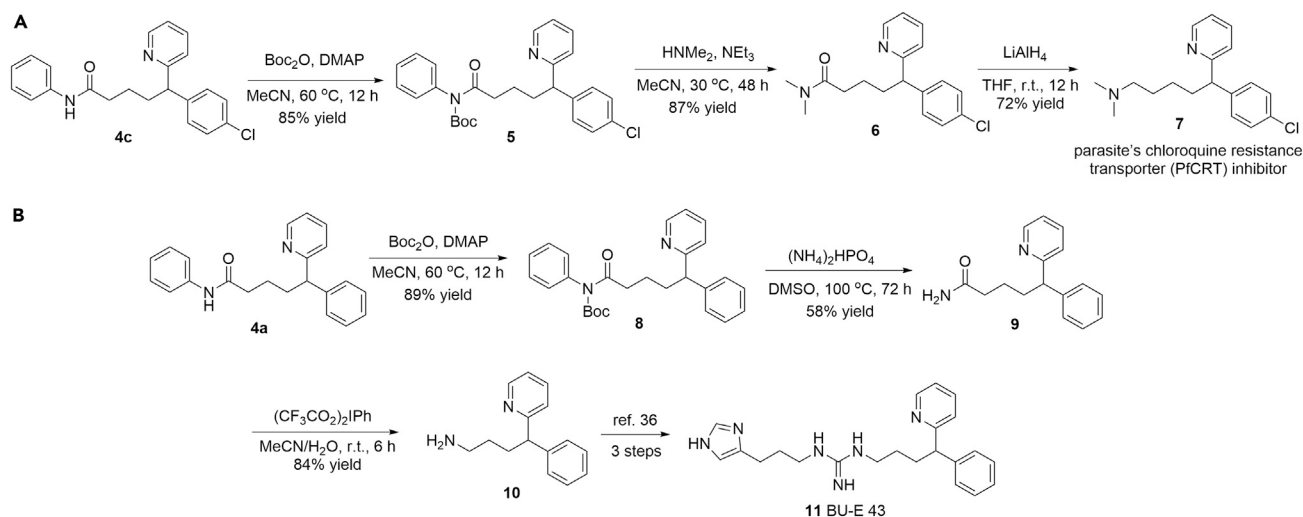


Figure 4. Transformations of coupling products

(A) Synthesis of parasite's chloroquine resistance transporter inhibitor 7.

(B) Formal synthesis of histamine H_2 receptor agonist BU-E 43 11.

reduction potential of **1ap** ($E_{p/2} = -1.64$ V vs. SCE). With 4DPAIPN as the photocatalyst, the homocoupling of acryloyl pyrazole proceeded smoothly at room temperature, delivering product **4ap** in moderate yield. The homocoupling reactions were also applicable to acrylamides bearing different α -substituents, such as methyl, benzyl, and phenyl groups (**4aq–4as**). Notably, indole-containing acrylamide turned out to be a good substrate, and the corresponding homocoupling product was smoothly formed (**4at**).

Synthetic utility

The aryl pyridine moieties are often found in bioactive molecules and approved drugs such as pheniramine and chlorphenamine. To illustrate the synthetic value of this alkene cross-coupling protocol, we elaborated the cross-coupling products that could form biologically significant molecules (Figure 4). *N*-Phenylamides can be readily converted to other amides through transamidation reactions,^{32,33} often via the introduction of a bulky protective group to destabilize the amide resonance. The Boc group was introduced into the coupling product (**4c**), forming an *N*-Boc protected amide (**5**) with a yield of 85%. A subsequent transamidation with dimethylamine furnished an *N,N*-dimethyl amide (**6**) with a yield of 87%. Finally, reduction with lithium aluminum hydride delivered an amine (**7**), which is a compound known to inhibit the parasite's chloroquine resistance transporter (PfCRT).³⁴ Similarly, a primary amide (**9**) was obtained through a few straightforward reactions. Ammonium hydrogen phosphate could be utilized as a convenient ammonia source, eliminating the use of volatile ammonia and pressure reactors. Treatment of the amide (**9**) with bis(trifluoroacetoxy)iodobenzene triggered a Hofmann rearrangement and furnished the primary amine (**10**),³⁵ the transformation of which into the histamine H_2 receptor agonist BU-E 43 (**11**) has been well established in the literature.³⁶

Proposed mechanisms

To determine the mechanisms of these reactions, we conducted the Stern-Volmer fluorescence quenching experiments with the two photocatalysts (Figure 5A). Oxalate quenched the fluorescence of both photocatalysts, while the hydrocarboxylated

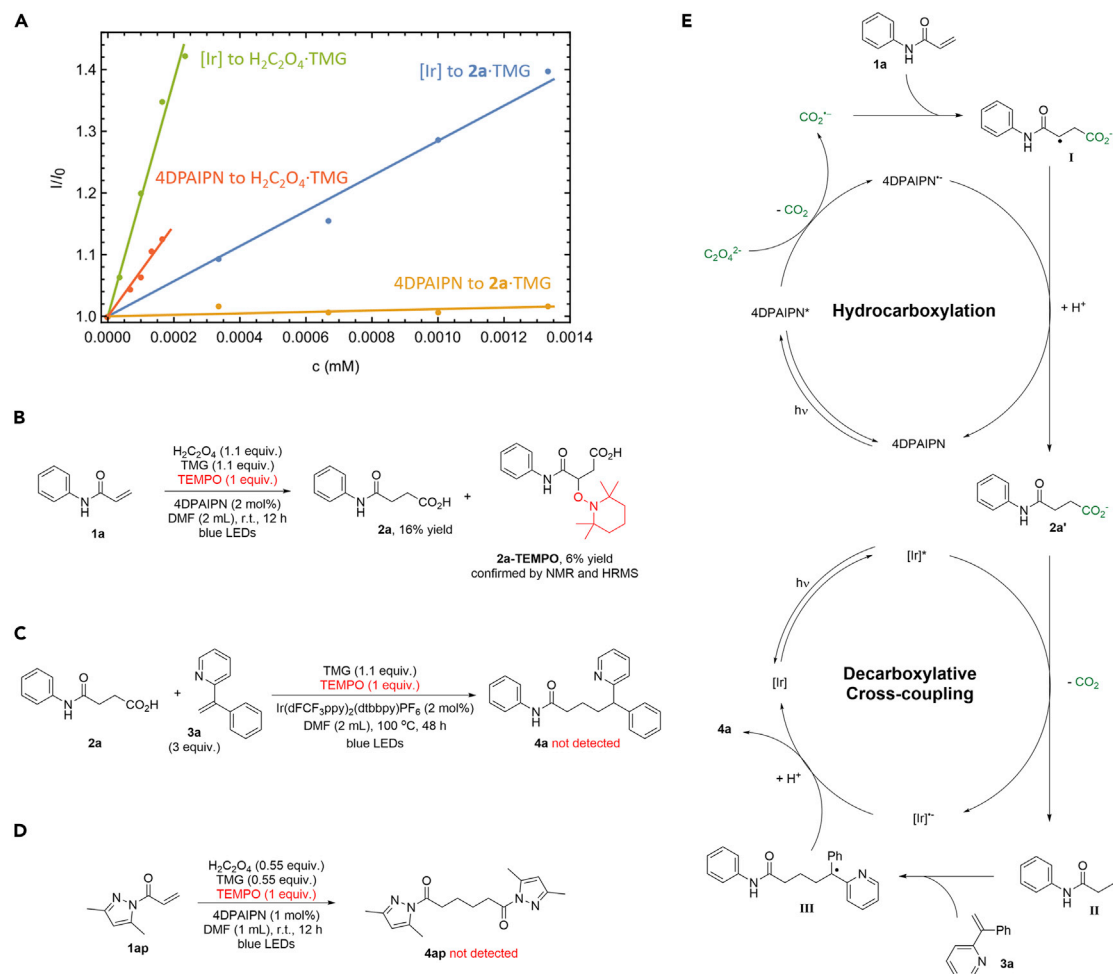


Figure 5. Mechanistic studies

- (A) Stern-Volmer fluorescence quenching experiments.
 (B) Radical scavenger experiments for hydrocarboxylation.
 (C) Radical scavenger experiments for decarboxylative cross-coupling.
 (D) Radical scavenger experiments for homocoupling.
 (E) Proposed mechanisms for cross-couplings.

product (**2a**·TMG) quenched only the fluorescence of $\text{Ir}(\text{dFCF}_3\text{ppy})_2(\text{dtbbpy})\text{PF}_6$. Given that under light irradiation, $\text{Ir}(\text{dFCF}_3\text{ppy})_2(\text{dtbbpy})\text{PF}_6$ ($E_{1/2}([\text{Ir}^*]/[\text{Ir}]^-) = 1.21 \text{ V vs. SCE}$)³⁷ is more oxidative than 4DPAIPN ($E_{1/2}(4\text{DPAIPN}^*/4\text{DPAIPN}^-) = 1.10 \text{ V vs. SCE}$)³⁸, these experiments reveal that $\text{Ir}(\text{dFCF}_3\text{ppy})_2(\text{dtbbpy})\text{PF}_6$ is able to oxidize both the oxalate ($E_{1/2}(\text{C}_2\text{O}_4^{\bullet-}/\text{C}_2\text{O}_4^{2-}) = 0.06 \text{ V vs. SCE}$) and the butyrate (**2a**) ($E_{p/2} = 1.0 \text{ V vs. SCE}$), but 4DPAIPN can efficiently oxidize only the oxalate and is thus unable to catalyze the decarboxylative cross-coupling reaction. In addition, the $\text{Ir}(\text{dFCF}_3\text{ppy})_2(\text{dtbbpy})\text{PF}_6$ photocatalyst was less effective in the hydrocarboxylation reaction because it led to overreaction. Therefore, the dual-photocatalyst system is crucial for the overall transformation by promoting the desired reactions at different stages.

The radical scavenger, 2,2,6,6-tetramethyl-1-piperidinyloxy (TEMPO), was employed to trap radical intermediates (Figures 5B and 5C). When one equivalent of TEMPO was added to the reaction system, the radical intermediate generated

from acrylamide (**1a**) and carbon dioxide radical anion was successfully trapped to form a TEMPO adduct (**2a**-TEMPO), indicating the radical nature of the addition reaction. The decarboxylative cross-coupling reaction was tested in the presence of TEMPO, and the formation of the cross-coupling product was completely suppressed. A TEMPO adduct was not detected, however, probably due to its instability at high temperatures. Additionally, the deuterium-labeling experiments for both steps also demonstrated that the reaction follows a Giese-type addition pathway (Figures S8 and S9).

The mechanism of homocoupling reaction was subsequently explored. Similarly, one molar equivalent of TEMPO completely suppressed homocoupling (Figure 5D), and the employment of deuterated oxalic acid produced deuterated diamide products with deuterium incorporation at the α -position of amides (Figure S10). Given that $\text{CO}_2^{\cdot-}$ ($E_{1/2}(\text{CO}_2/\text{CO}_2^{\cdot-}) = -2.2$ V vs. SCE) is capable of reducing acrylamide **1ap** ($E_{p/2} = -1.64$ V vs. SCE), while the photocatalyst ($E_{1/2}(4\text{DPAIPN}/4\text{DPAIPN}^-) = -1.52$ V vs. SCE)³⁸ is not a sufficiently powerful reducing agent, homocoupling was likely to proceed through a radical addition pathway. Moreover, the ionic repulsion between two transient radical anion species derived from acrylamide also makes the radical-radical coupling pathway unlikely.

Based on these mechanistic studies, a plausible mechanism for cross-coupling is illustrated in Figure 5E. In the hydrocarboxylation step, oxalate is first oxidized by light-excited 4DPAIPN, generating the carbon dioxide radical anion, which adds to acrylamide (**1a**) to form an intermediate (I). A reduction and protonation process furnishes the hydrocarboxylated intermediate (**2a**), which readily undergoes the decarboxylative cross-coupling reaction. After the introduction of $\text{Ir}(\text{dFCF}_3\text{ppy})_2(\text{dtbbpy})\text{PF}_6$ and the coupling partner (**3a**), the decarboxylative cross-coupling reaction takes place. The oxidation of carboxylate (**2a'**) by excited $\text{Ir}(\text{dFCF}_3\text{ppy})_2(\text{dtbbpy})\text{PF}_6$, followed by decarboxylation, forms the active primary radical (II). This radical intermediate is trapped by alkene (**3a**), and finally, reduction and protonation deliver the cross-coupling product (**4a**). A plausible mechanism for the homocoupling was also proposed (Figure S17).

Conclusion

We have developed an efficient protocol utilizing oxalic acid as a traceless linchpin for the convenient reductive cross-coupling of two simple alkene reaction partners. The reaction makes use of a dual-photocatalyst system and merges two separate reaction steps, a hydrocarboxylation reaction and a decarboxylative addition reaction, into a one-pot process. We demonstrated the practical value of this cross-coupling reaction by facile synthesis of biologically significant molecules. In view of the ubiquitous presence of alkene functionality in organic molecules, a general traceless cross-coupling process that involves simple alkenes as reaction partners adds a powerful tool to the synthetic organic chemists' arsenal. The facile and mild generation of the CO_2 radical anion from oxalic acid through photoredox catalysis disclosed herein will pave the way to the broad utilization of this reactive intermediate in the synthesis of fine chemicals.

EXPERIMENTAL PROCEDURES

Resource availability

Lead contact

Further information and requests for resources should be directed to and will be fulfilled by the lead contact, Yixin Lu (chmlyx@nus.edu.sg).

Materials availability

All materials generated in this study are available from the lead contact without restriction.

Data and code availability

The crystal structures of the product **4a** in this article have been deposited in the Cambridge Crystallographic Data Center under the accession number CCDC: 2193902.

SUPPLEMENTAL INFORMATION

Supplemental information can be found online at <https://doi.org/10.1016/j.chempr.2022.12.013>.

ACKNOWLEDGMENTS

J.W. thanks the Ministry of Education (MOE) of Singapore (MOET2EP10120-0014). Y.L. thanks the Singapore National Research Foundation, Prime Minister's Office for the NRF Investigatorship Award (A-0004067-00-02). Financial support from the Ministry of Education (MOE) of Singapore (A-0008481-00-00) is also acknowledged.

AUTHOR CONTRIBUTIONS

Y.L. and J.W. initiated and supervised the project; Z.W. designed the experiments; Z.W., M.W., and K.Z. conducted the experiments; all authors analyzed and discussed the experiment data; Y.L., J.W., and Z.W. wrote the manuscript and [supplemental information](#).

DECLARATION OF INTERESTS

We have submitted a provisional patent related to this work.

Received: September 19, 2022

Revised: November 22, 2022

Accepted: December 14, 2022

Published: January 16, 2023

REFERENCES

1. Botte, G.G. (2014). Electrochemical manufacturing in the chemical industry. *Electrochem. Soc. Interface* 23, 49–55. <https://doi.org/10.1149/2.F04143if>.
2. Hoveyda, A.H., and Zhugralin, A.R. (2007). The remarkable metal-catalysed olefin metathesis reaction. *Nature* 450, 243–251. <https://doi.org/10.1038/nature06351>.
3. Ogba, O.M., Warner, N.C., O'Leary, D.J., and Grubbs, R.H. (2018). Recent advances in ruthenium-based olefin metathesis. *Chem. Soc. Rev.* 47, 4510–4544. <https://doi.org/10.1039/C8CS00027A>.
4. Ho, C.-Y., Chan, C.-W., and He, L. (2015). Catalytic asymmetric hydroalkenylation of vinylarenes: electronic effects of substrates and chiral N-heterocyclic carbene ligands. *Angew. Chem. Int. Ed. Engl.* 54, 4512–4516. <https://doi.org/10.1002/anie.201411882>.
5. RajanBabu, T.V. (2003). Asymmetric hydrovinylation reaction. *Chem. Rev.* 103, 2845–2860. <https://doi.org/10.1021/cr020040g>.
6. Rajanbabu, T.V. (2009). In pursuit of an ideal C–C bond-forming reaction: development and applications of the hydrovinylation of olefins. *Synlett* 2009, 853–885. <https://doi.org/10.1055/s-0028-1088213>.
7. Hatamoto, Y., Sakaguchi, S., and Ishii, Y. (2004). Oxidative cross-coupling of acrylates with vinyl carboxylates catalyzed by a Pd(OAc)₂/HPMoV/O₂ system. *Org. Lett.* 6, 4623–4625. <https://doi.org/10.1021/ol047971u>.
8. Wen, Z.K., Xu, Y.H., and Loh, T.P. (2013). Palladium(ii)-catalyzed cross-coupling of simple alkenes with acrylates: a direct approach to 1,3-dienes through C–H activation. *Chem. Sci.* 4, 4520–4524. <https://doi.org/10.1039/c3sc52275j>.
9. Liang, Q.-J., Yang, C., Meng, F.-F., Jiang, B., Xu, Y.-H., and Loh, T.-P. (2017). Chelation versus non-chelation control in the stereoselective alkenyl sp² C–H bond functionalization reaction. *Angew. Chem. Int. Ed. Engl.* 56, 5091–5095. <https://doi.org/10.1002/anie.201700559>.
10. Jiang, B., Zhao, M., Li, S.S., Xu, Y.H., and Loh, T.P. (2018). Macrolide synthesis through intramolecular oxidative cross-coupling of alkenes. *Angew. Chem. Int. Ed. Engl.* 57, 555–559. <https://doi.org/10.1002/ange.201710601>.
11. Meng, K., Sun, Y., Zhang, J., Zhang, K., Ji, X., Ding, L., and Zhong, G. (2019). Iridium-catalyzed cross-coupling reactions of alkenes by hydrogen transfer. *Org. Lett.* 21, 8219–8224. <https://doi.org/10.1021/acs.orglett.9b02935>.
12. Li, T., Shen, C., Sun, Y., Zhang, J., Xiang, P., Lu, X., and Zhong, G. (2019). Cobalt-catalyzed olefinic C–H alkenylation/alkylation switched by carbonyl groups. *Org. Lett.* 21, 7772–7777. <https://doi.org/10.1021/acs.orglett.9b02717>.
13. Lo, J.C., Yabe, Y., and Baran, P.S. (2014). A practical and catalytic reductive olefin coupling. *J. Am. Chem. Soc.* 136, 1304–1307. <https://doi.org/10.1021/ja4117632>.
14. Lo, J.C., Gui, J., Yabe, Y., Pan, C.-M., and Baran, P.S. (2014). Functionalized olefin cross-coupling to construct carbon–carbon bonds.

- Nature 516, 343–348. <https://doi.org/10.1038/nature14006>.
- Streuff, J. (2011). A titanium(III)-catalyzed redox umpolung reaction for the reductive cross-coupling of enones with acrylonitriles. *Chemistry* 17, 5507–5510. <https://doi.org/10.1002/chem.201100501>.
 - Kong, M., Tan, Y., Zhao, X., Qiao, B., Tan, C.-H., Cao, S., and Jiang, Z. (2021). Catalytic reductive cross coupling and enantioselective protonation of olefins to construct remote stereocenters for azaarenes. *J. Am. Chem. Soc.* 143, 4024–4031. <https://doi.org/10.1021/jacs.1c01073>.
 - Farrell, M., Melillo, B., and Smith, A.B., III (2016). Type II anion relay chemistry: exploiting bifunctional Weinreb amide linchpins for the one-pot synthesis of differentiated 1,3-diketones, pyrans, and spiroketals. *Angew. Chem. Int. Ed. Engl.* 55, 232–235. <https://doi.org/10.1002/ange.201509342>.
 - Wang, X., Yang, M., Ye, S., Kuang, Y., and Wu, J. (2021). S(vi) in three-component sulfonamide synthesis: use of sulfuric chloride as a linchpin in palladium-catalyzed Suzuki–Miyaura coupling. *Chem. Sci.* 12, 6437–6441. <https://doi.org/10.1039/D1SC01351C>.
 - Filippini, D., and Silvi, M. (2022). Visible light-driven conjunctive olefination. *Nat. Chem.* 14, 66–70. <https://doi.org/10.1038/s41557-021-00807-x>.
 - Kapoor, M., Liu, D., and Young, M.C. (2018). Carbon dioxide-mediated C(sp³)–H arylation of amine substrates. *J. Am. Chem. Soc.* 140, 6818–6822. <https://doi.org/10.1021/jacs.8b05061>.
 - Kapoor, M., Chand-Thakuri, P., and Young, M.C. (2019). Carbon dioxide-mediated C(sp²)–H arylation of primary and secondary benzylamines. *J. Am. Chem. Soc.* 141, 7980–7989. <https://doi.org/10.1021/jacs.9b03375>.
 - Ye, J., Kalvet, I., Schoenebeck, F., and Rovis, T. (2018). Direct α -alkylation of primary aliphatic amines enabled by CO₂ and electrostatics. *Nat. Chem.* 10, 1037–1041. <https://doi.org/10.1038/s41557-018-0085-9>.
 - McMurray, L., McGuire, T.M., and Howells, R.L. (2020). Recent advances in photocatalytic decarboxylative coupling reactions in medicinal chemistry. *Synthesis* 52, 1719–1737. <https://doi.org/10.1055/s-0039-1690843>.
 - Kitcatt, D.M., Nicolle, S., and Lee, A.-L. (2022). Direct decarboxylative giese reactions. *Chem. Soc. Rev.* 51, 1415–1453. <https://doi.org/10.1039/D1CS01168E>.
 - Schuler, E., Demetriou, M., Shiju, N.R., and Gruter, G.M. (2021). Towards sustainable oxalic acid from CO₂ and biomass. *ChemSusChem.* 14, 3636–3664. <https://doi.org/10.1002/cssc.202101272>.
 - Hendy, C.M., Smith, G.C., Xu, Z., Lian, T., and Jui, N.T. (2021). Radical chain reduction via carbon dioxide radical anion (CO₂^{•-}). *J. Am. Chem. Soc.* 143, 8987–8992. <https://doi.org/10.1021/jacs.1c04427>.
 - Seo, H., Katcher, M.H., and Jamison, T.F. (2017). Photoredox activation of carbon dioxide for amino acid synthesis in continuous flow. *Nat. Chem.* 9, 453–456. <https://doi.org/10.1038/nchem.2690>.
 - Alektiar, S.N., and Wickens, Z.K. (2021). Photoinduced hydrocarboxylation via thiol-catalyzed delivery of formate across activated alkenes. *J. Am. Chem. Soc.* 143, 13022–13028. <https://doi.org/10.1021/jacs.1c07562>.
 - Chmiel, A.F., Williams, O.P., Chernowsky, C.P., Yeung, C.S., and Wickens, Z.K. (2021). Non-innocent radical ion intermediates in photoredox catalysis: parallel reduction modes enable coupling of diverse aryl chlorides. *J. Am. Chem. Soc.* 143, 10882–10889. <https://doi.org/10.1021/jacs.1c05988>.
 - Kai, T., Zhou, M., Johnson, S., Ahn, H.S., and Bard, A.J. (2018). Direct observation of C₂O₄^{•-} and CO₂^{•-} by oxidation of oxalate within nanogap of scanning electrochemical microscope. *J. Am. Chem. Soc.* 140, 16178–16183. <https://doi.org/10.1021/jacs.8b08900>.
 - AlSalka, Y., Al-Madanat, O., Curti, M., Hakki, A., and Bahnmann, D.W. (2020). Photocatalytic H₂ evolution from oxalic acid: effect of cocatalysts and carbon dioxide radical anion on the surface charge transfer mechanisms. *ACS Appl. Energy Mater.* 3, 6678–6691. <https://doi.org/10.1021/acsaem.0c00826>.
 - Liu, Y., Shi, S., Achtenhagen, M., Liu, R., and Szostak, M. (2017). Metal-free transamidation of secondary amides via selective N–C cleavage under mild conditions. *Org. Lett.* 19, 1614–1617. <https://doi.org/10.1021/acs.orglett.7b00429>.
 - Chen, J., Xia, Y., and Lee, S. (2020). Transamidation for the synthesis of primary amides at room temperature. *Org. Lett.* 22, 3504–3508. <https://doi.org/10.1021/acs.orglett.0c00958>.
 - Deane, K.J., Summers, R.L., Lehane, A.M., Martin, R.E., and Barrow, R.A. (2014). Chlorpheniramine analogues reverse chloroquine resistance in *Plasmodium falciparum* by inhibiting PfCRT. *ACS Med. Chem. Lett.* 5, 576–581. <https://doi.org/10.1021/ml5000228>.
 - Loudon, G.M., Radhakrishna, A.S., Almond, M.R., Blodgett, J.K., and Boutin, R.H. (1984). Conversion of aliphatic amides into amines with [I, I-bis(trifluoroacetoxy)iodo] benzene. 1. Scope of the reaction. *J. Org. Chem.* 49, 4272–4276. <https://doi.org/10.1021/jo00196a031>.
 - Buschauer, A. (1989). Synthesis and in vitro pharmacology of arpromidine and related phenyl(pyridylalkyl)guanidines, a potential new class of positive inotropic drugs. *J. Med. Chem.* 32, 1963–1970. <https://doi.org/10.1021/jm00128a045>.
 - Prier, C.K., Rankic, D.A., and MacMillan, D.W.C. (2013). Visible light photoredox catalysis with transition metal complexes: applications in organic synthesis. *Chem. Rev.* 113, 5322–5363. <https://doi.org/10.1021/cr300503r>.
 - Luo, J., and Zhang, J. (2016). Donor–acceptor fluorophores for visible-light-promoted organic synthesis: photoredox/Ni dual catalytic C(sp³)–C(sp²) cross-coupling. *ACS Catal.* 6, 873–877. <https://doi.org/10.1021/acscatal.5b02204>.